TROPICAL LIFE SCIENCES RESEARCH

Virtual Screening, Molecular Docking, and Molecular Dynamics Simulation of Bioactive Compounds from Various Indonesian Medicinal Plants as Potential Inhibitors of Human Papillomavirus Type 16 E6 Protein in Cervical Cancer Development

Authors:

Arief Hidayatullah, Diana Widiastuti, Wira Eka Putra*, Muhaimin Rifa'i, Muhammad Fikri Heikal and Sustiprijatno

*__Correspondence:__ wira.putra.fmipa@um.ac.id

Submitted: 10 September 2021; **Accepted:** 2 October 2024; **Early view:** 18 December 2024

To cite this article: Arief Hidayatullah, Diana Widiastuti, Wira Eka Putra, Muhaimin Rifa'i, Muhammad Fikri Heikal, and Sustiprijatno. (in press). Virtual screening, molecular docking, and molecular dynamics simulation of bioactive compounds from various Indonesian medicinal plants as potential inhibitors of human papillomavirus type 16 E6 protein in cervical cancer development. *Tropical Life Sciences Research.*

Highlights

- The E6 protein serves as a pivotal oncoprotein implicated in the progression of cancer.
- Asarinin and thiazolo[3,2-a]benzimidazole-3(2H)-one,2-(2-fluorobenzylideno)-7,8-dimethyl demonstrated strong affinity and stable interaction against HPV16 E6 protein.
- Asarinin and thiazolo[3,2-a]benzimidazole-3(2H)-one,2-(2-fluorobenzylideno)-7,8-dimethyl were predicted to be the most effective compounds for HPV16 E6 protein inhibitor candidate.

Virtual Screening, Molecular Docking, and Molecular Dynamics Simulation of Bioactive Compounds from Various Indonesian Medicinal Plants as Potential Inhibitors of Human Papillomavirus Type 16 E6 Protein in Cervical Cancer Development

[1]Arief Hidayatullah, [2]Diana Widiastuti, [3]Wira Eka Putra*, [4]Muhaimin Rifa'i, [5]Muhammad Fikri Heikal and [6]Sustiprijatno

[1]Health Governance Initiative, United Nations Development Programme Indonesia, Eijkman-RSCM Building, Jakarta, Indonesia
[2]Departmentof Chemistry, Faculty of Mathematics and Natural Science, Universitas Pakuan, West Java, Indonesia
[3]Biotechnology Study Program, Department of Applied Sciences, Faculty of Mathematics and Natural Sciences, Universitas Negeri Malang, East Java, Indonesia
[4]Department of Biology, Faculty of Mathematics and Natural Sciences, Brawijaya University, East Java, Indonesia
[5]Department of Biology, Faculty of Mathematics and Natural Sciences, Universitas Negeri Malang, East Java, Indonesia
[6]Research Center for Applied Botany, National Research and Innovation Agency, West Java, Indonesia

*Corresponding author: wira.putra.fmipa@um.ac.id

Running head: Bioinformatics Study of Anti-Viral Drug

Submitted: 10 September 2021; **Accepted:** 2 October 2024; **Early view:** 18 December 2024

To cite this article: Arief Hidayatullah, Diana Widiastuti, Wira Eka Putra, Muhaimin Rifa'i, Muhammad Fikri Heikal, and Sustiprijatno. (in press). Virtual screening, molecular docking, and molecular dynamics simulation of bioactive compounds from various Indonesian medicinal plants as potential inhibitors of human papillomavirus type 16 E6 protein in cervical cancer development. *Tropical Life Sciences Research.*

Abstract. Infection of keratinocytes by high-risk HPV strains, notably HPV16, is responsible for the onset of cervical cancer. The E6 protein serves as a pivotal oncoprotein implicated in the progression of cancer. We utilized a virtual screening method to identify bioactive compounds in a variety of commonly used medicinal plants in Indonesia. All the top five compounds bind to a single binding site on the E6 major hydrophobic groove, which corresponds to the binding site for the E6AP and IRF3's LxxLL motifs. They are expected to function as competitive inhibitors, inhibiting the development of the E6-E6AP and E6-IRF3 complexes, which limit p53 degradation and therefore cell proliferation, thus preserving the innate immune response to HPV16 infection. Asarinin and thiazolo[3,2-a]benzimidazole-3(2H)-one,2-(2-fluorobenzylideno)-7,8-dimethyl were predicted to be the most effective compounds in this research owing to their strong affinity for and persistent interactions with the E6 major hydrophobic groove, particularly in comparison to pharmacological controls.

Keywords: Cervical Cancer, Dynamics Simulation, E6 Protein, HPV16, Molecular Docking

INTRODUCTION

Human Papillomavirus, or HPV, constitutes a cluster of non-enveloped DNA viruses that specifically assemble within the nucleus and predominantly target the basal layer of keratinocytes. Its transmission primarily occurs through skin-to-skin contact, notably via sexual contact (Bonnez 2009; Forcier & Musacchio 2010; Tao *et al.* 2003). Presently, there exist over 200 identified types of HPV, categorized generally into five genotype groups (α, β, γ, μ and ν) and classified into two risk categories: High-risk (HR) and Low-risk (LR) HPV (Bzhalava *et al.* 2013; Cobo 2012; Graham 2017). LR-HPV infections, responsible for the majority of HPV cases, are generally asymptomatic and pose no significant health risks. The primary manifestation of these infections is the development of skin warts on various body parts including the hands, feet, and genital area. Conversely, HR-HPV infections, stemming from HPV types 16, 18, 31, 35, 39, 45, 51, 56, 59, 68, 73, and 82, serve as the principal precursors to anogenital cancers, with cervical cancer being the most prevalent among them (Bzhalava *et al.* 2013; Doorbar *et al*. 2012; Graham 2017; Tyring *et al.* 2016). Cervical cancer stands as one of the most prevalent malignancies affecting women globally. In Indonesia specifically, cervical cancer ranks as the second most common cancer following breast cancer, boasting a prevalence rate ranging between 43.3 and 52.4 cases per 100,000 individuals (Arbyn *et al.* 2020; Putri *et al.* 2019; Wahidin *et al.* 2020; Zhang *et al.* 2020). Around 70-90% of cervical cancer instances arise from infections attributed to HPV 16 and HPV 18, two prominent high-risk HPV strains. Notably, HPV 16 alone is responsible for approximately 55% of all cervical cancer cases *(Graham 2017; Huibregtse et al. 1993; Tan et al. 2012; Wang et al.* 2018).

Regarding the extensively studied HPV type, HPV 16, its viral genome comprises two distinct categories of genes. The early genes, which encompass the primary nonstructural proteins (E1, E2, E4, E5, E6, and E7), play pivotal roles in orchestrating the replication and maturation phases of HPV within host cells. Conversely, the late gene primarily oversees the assembly of mature virion structure, serving as the principal structural proteins (L1 and L2). Among those nonstructural proteins, one of the most studied is the E6 protein. The E6 protein is one of the critical oncoproteins that differentiate HR and LR variants of HPV (Doorbar et al. 2012; Egawa & Doorbar 2017; Graham 2017; Underbrink et al. 2016). In alpha-HR-HPV such as HPV16, this specific protein will inhibit the transactivation process and degradation of p53 using its 26S proteasome for degradation, causing DNA damage resulting in immortalization of infected cells, leading to cancer development (Bernard et al. 2011; Doorbar et al. 2012; Scheurer et al. 2005). In addition, E6 is also known to inhibit innate immune responses to infected cells by inhibiting IRF3 and TYK2 signaling mechanisms (Gutiérrez-Hoya & Soto-Cruz 2020; Reiser et al. 2011; Tummers & van der Burg 2015). In its mechanism of action as an oncoprotein, E6 forms a dimer with E6-associated protein (E6AP) or IRF3 (Doorbar et al. 2012; M. Shah et al. 2013; Tummers & van der Burg 2015; Zanier et al. 2014). Interaction between E6 protein and E6AP is very crucial in the mechanism of cell immortalization and cancer development; meanwhile, the E6 protein also binds to IRF3 and prevents its transcriptional activity, mainly the IFN-β mRNA synthesis, crucial to silence the innate immune responses (Ronco et al., 1998; Tummers & van der Burg, 2015). We aimed to avoid this kind of formation through intervention by antiviral compounds that are competitive against E6AP and IRF3 (Reiser et al. 2011; Tan et al. 2012; Tummers & van der Burg 2015). Several anti-cancer drugs have E6 suppressant effects based on *in vitro* studies, including vorinostat and mitomycin C. Vorinostat functions as a competitive inhibitor at the E6 binding site of p53, while also downregulating the E6 protein itself in HPV-positive cervical cancer cells. As a pan-HDAC inhibitor, vorinostat exerts its effects by significantly reducing the activities of both E6

and E7 oncoproteins, crucial players in HPV-induced carcinogenesis. Additionally, vorinostat has been found to disrupt viral DNA amplification and inhibit host DNA replication, further impeding the progression of HPV-associated cervical cancer (Banerjee et al. 2018; Z. Lin et al. 2009; Tan et al. 2012). Mitomycin C exerts its effects as a DNA alkylating agent, which leads to the suppression of E6 protein expression and disrupts its downstream effects. Specifically, mitomycin C is thought to inhibit the E6-activated RSV (Rous sarcoma virus) promoter. However, the precise mechanism by which mitomycin C achieves this inhibition is still not fully elucidated (Kang et al. 2010; Vande Pol & Klingelhutz 2013). A study mention that it could hinders the degradation process of p53, a tumor suppressor protein that is targeted for degradation by the E6 protein in HPV-infected cells (White et al. 2014).

Indonesia, being one of the largest tropical countries, hosts a rich diversity of over 7000 species of medicinal plants. Despite this vast wealth, less than 10% of these species are officially acknowledged as phytopharmaceuticals (Salim & Munadi 2017). Throughout Indonesian culture, numerous medicinal plants have been utilized for centuries to manage or alleviate a spectrum of diseases, drawing upon empirical knowledge within communities. However, scientific substantiation for their efficacy sometimes remains limited (Jennifer & Saptutyningsih 2015; Sumayyah & Salsabila 2017). Around 55% of Indonesians use traditional medicines daily, and more than 95% of them thought they feel the benefits of these medicines (Jennifer & Saptutyningsih 2015; Sumayyah & Salsabila 2017). Those open up great opportunities for the exploration of drug candidates for many diseases, including HR-HPV infection. Drug design research would be long-continuous research, primarily if the ingredients used are natural-based. One of the earliest stages is the screening compound and trial based in silico as in this study (Putra et al. 2017; Kitchen et al. 2004; Lionta et al. 2014; Putra et al. 2020). Specifically, this study aims to explore potential anti-HPV E6 compounds derived from natural ingredients outside of the rhizome group because most research on herbal medicines and their uses has focused on them (Beers 2012; Hakim 2015; Kristianto et al. 2020; Woerdenbag & Kayser 2014). Preliminary studies showed 476 bioactive compounds from 18 non-rhizome simplicia that could be tested through virtual screening against HPV16 E6 protein (Abdallah et al. 2016; Abdel-Moneim et al. 2013; Amalina A et al. 2013; Anwar et al. 2009; Asika et al. 2016; Badgujar et al. 2014; Beyzi et al. 2017; Choi et al. 2016; Chung 2009; Dilla Dertyasasa & Anindito Sri Tunjung 2017; Ekpenyong et al. 2015; El-Saber Batiha et al. 2020; Fagodia et al. 2017; Figueirinha et al. 2008; González-Molina et al. 2010; Kadam & Lele 2017; Laribi et al. 2015; Li et al. 2017; Mahmood et al. 2016; Majdi et al. 2020; Mohammed et al. 2016; Pandey et al. 2016; Patil et al. 2009; Patra et al. 2020; Piras et al. 2013; Rattanachaikunsopon & Phumkhachorn 2010; G. Shah et al. 2011; Srivastava et al. 2005; Sukandar et al. 2016; Umaru et al. 2020; Wei et al. 2019; Yahia et al. 2020; Zahra & Iskandar 2017).

MATERIALS AND METHODS

Data Retrieval

This research was aimed to target the HPV 16 E6 oncoprotein. The target protein's amino acid sequence was obtained from UniProt (https://www.uniprot.org/uniprot) with ID P03126. The 3D structure of protein was modeled using I-TASSER webserver (https://zhanglab.dcmb.med.umich.edu/I-TASSER/). The 3D modeled was chosen based on the rank of generated model, with highest C-score value and TM-score. The compound data used comes from various types of plants commonly consumed in Indonesia. There are 476 bioactive compounds derived from 18 plant sources known to have antiviral, antibacterial, antifungal, and

antimicrobial properties (Abdallah et al. 2016; Abdel-Moneim et al. 2013; Amalina A et al. 2013; Anwar et al. 2009; Asika et al. 2016; Badgujar et al. 2014; Beyzi et al. 2017; Choi et al. 2016; Chung 2009; Dilla Dertyasasa & Anindito Sri Tunjung 2017; Ekpenyong et al. 2015; El-Saber Batiha et al. 2020; Fagodia et al. 2017; Figueirinha et al. 2008; González-Molina et al. 2010; Kadam & Lele 2017; Laribi et al. 2015; Li et al. 2017; Mahmood et al. 2016; Majdi et al. 2020; Mohammed et al. 2016; Pandey et al. 2016; Patil et al. 2009; Patra et al. 2020; Piras et al. 2013; Rattanachaikunsopon & Phumkhachorn 2010; G. Shah et al. 2011; Srivastava et al. 2005; Sukandar et al. 2016; Umaru et al. 2020; Wei et al. 2019; Yahia et al. 2020; Zahra & Iskandar 2017). The structure of all these potential compounds mined from PubChem (https://pubchem.ncbi.nlm.nih.gov/) in SDF format (Putra *et al.* 2023; Putra 2018). There are two drug compounds used as controls in this study, vorinostat (CID: 5311) and mitomycin C (CID: 5746), currently used in cervical cancer therapy. Those drugs were also downloaded for their 3D structure in the SDF format.

Drug-likeness Screening

All gathered compounds underwent testing against the Lipinski rule of five parameters to evaluate their pharmacological characteristics as our previous study (Hidayatullah et al. 2021; Putra & Rifa'i 2020). The Lipinski test was conducted utilizing the Supercomputing Facility for Bioinformatics and Computational Biology at IT Delhi server (http://www.scfbio-iitd.res.in/software/drugdesign/lipinski.jsp) (Jayaram *et al.* 2012). Subsequently, all potential compounds meeting Lipinski's criteria will be subjected to minimization and converted to the AutoDock format using the PyRx program integrated with the OpenBabel GUI (Mirzaei *et al.* 2015).

Molecular Docking Process

The docking procedure is conducted utilizing AutoDock Vina, integrated with PyRx (https://pyrx.sourceforge.io/) (Trott & Olson 2009). Our docking protocol encompasses the entire structure of the target protein. The molecular coverage area is delineated by dimensions of 44.4289 × 38.7535 × 71.0904 Angstroms, with a central coordinate set at 63.4878 × 63.4683 × 56.2079. The primary docking outcomes include the compound's affinity expressed in kcal/mol, the location of the binding site, and the subsequent visualization of protein-ligand interactions (Widiastuti *et al.* 2023; Putra *et al.* 2021).

Visualization Process

The visualization procedure comprises two distinct stages: initially, a 3D visualization is employed to gain a comprehensive understanding of potential compound binding sites on the E6 protein. Subsequently, a 2D visualization is employed to discern interactions within each protein-ligand complex (Hidayatullah et al. 2020; Putra et al. 2019). The 3D visualization step is executed utilizing PyMOL (https://pymol.org/2/), while the 2D visualization step is conducted utilizing LigPlot+ 2.1 (https://www.ebi.ac.uk/thornton-srv/software/LigPlus/).

Molecular Dynamics Simulation

Ligands exhibiting the lowest binding affinity scores were chosen for molecular dynamics (MD) simulation against the E6 protein. Simulation parameters were configured to mirror normal physiological conditions, including a temperature of 37°C, pressure of 1 atm, pH of 7.4, and a salt

content of 0.9%. The MD simulation was conducted for a duration of 1000 picoseconds. The simulation process was executed using the md_run macro program, followed by subsequent analysis utilizing md_analyze and md_analyeres (Hidayatullah et al. 2023).

RESULTS

The molecular docking results revealed that the top five compounds tested exhibited affinity values surpassing those of the two drug controls (mitomycin C; -6.4 kcal/mol, vorinostat; -6.7 kcal/mol). Specifically, the top five compounds identified are asarinin, thiazolo[3,2-a]benzimidazol-3(2H)-one,2-(2-fluorobenzylideno)-7,8-dimethyl, ellagic acid, magnoflorine, and galbacin. These compounds demonstrated affinities ranging from -7.8 to -8.2 kcal/mol, approximately 19-25% lower than both controls (Fig. 1).

Both 2D and 3D visualization outcomes depict that all of the top 5 compounds and controls were localized within a singular binding site. This binding site is situated adjacent to the main helix of the target protein, believed to be the binding site of the LxxLL motif of E6AP and IRF3 (Fig. 2). The dominant interaction formed in protein-ligand complexes is hydrophobic contact, with 86.5% of all interactions formed. Hydrogen bonds are only found in two potential compounds, namely ellagic acid, magnoflorine and drug controls. The hydrogen bonds formed by ellagic acid and magnoflorine have donor-acceptor distances ranging from 2.67-3.03Å and 2.94Å. The hydrogen bonds formed on vorinostat and mitomycin C have donor-acceptor distances ranging from 2.77-3.10Å and 3.13-3.16Å, respectively (Table 2; Fig. 3).

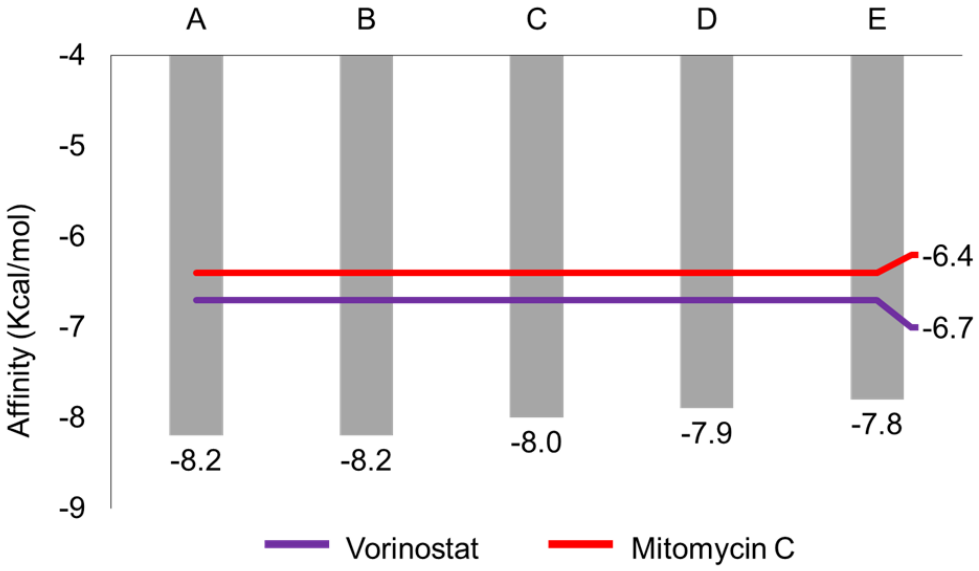

Figure 1. The affinity values of the top five compounds and controls, as determined by the docking results, are (A) asarinin, (B) thiazolo[3,2-a]benzimidazol-3(2H)-one, 2-(2-fluorobenzylideno)-7,8-dimethyl, (C) ellagic acid, (D) magnoflorine, and (E) galbacin.

Based on the identification results, the E6 protein from various sources exhibits three main residue groups associated with E6AP binding: the E6AP binding pocket, E6 pocket, and primary alpha helix residue (Table 1). Interestingly, there are interconnections among these residue groups, suggesting their involvement in forming the E6AP binding site. Specifically, the residues within the E6 pocket are found to be part of the E6AP binding pocket. Additionally, Leu74 and

Ser78, classified as primary alpha helix residues, are identified to interact directly with E6AP. Notably, Tyr77 is a residue that is part of all three groups simultaneously. Furthermore, the identification of IRF3's LxxLL binding site reveals that this motif's binding site aligns perfectly with the E6AP binding pocket (Table 1).

Table 1. Identification result of critical binding site and residues of HPV16 E6 protein.

Residues group	E6 residues
E6AP binding pocket	Arg17, Lys18, Val38, Tyr39, Asp56, Leu57, Val60, Arg62, Val69, Leu74, Tyr77, Ser78, Ile80, Ser81, Arg84, His85, Ser87, Tyr88, Gln98, Gln99, Leu107, Arg109, Glu114, Asn134, Ile135, Arg136, Gly137, Arg138 (M. Shah et al. 2013)
E6 pocket	Arg62, Arg17, Arg109, Arg136, Arg138, Arg84, Tyr77 (Ricci-López et al. 2019)
Main alpha helix	Lys72, Cys73, Leu74, Lys75, Phe76, Tyr77, Ser78, Lys79, Ile80, Ser81, Glu82, Tyr83, Arg84, His85 (Rietz et al. 2016; Vande Pol & Klingelhutz 2013
IRF3 binding pocket	Lys18, Val38, Tyr39, Leu57, Val60, Arg62, Val69, Leu74, Tyr77, Ser78, Ile8 Ser81, Arg84, His85, Arg109, Glu114, Arg138 (M. Shah et al. 2013)

The results of 2D visualization (Table 2; Fig. 4) highlight several conserved residues, including Arg138, Ser81, Gln114, Ser78, and Tyr77. Specifically, Ser81 and Gln114 are identified as binding site residues of E6AP (cyan), while Ser78 and Tyr77 are residues of the main helix structure (red), and Arg138 belongs to the E6 pocket (green). Interestingly, these residues exhibit overlap among the three groups; for instance, Arg138, besides being part of the E6 pocket, also contributes to the E6AP binding pocket, while Tyr77 is involved in both the E6 pocket and E6AP binding pocket, as well as the main helix structure. Additionally, the 2D visualization results indicate that 89% of the residues interacting with the target protein are E6AP binding pocket residues. Notably, asarinin, the compound with the highest affinity, interacts most extensively with target protein residues compared to other potential compounds and drug controls (involving 12 residues). Overall, the analysis suggests that the residues associated with potential compounds and drug controls share more than 80% identity.

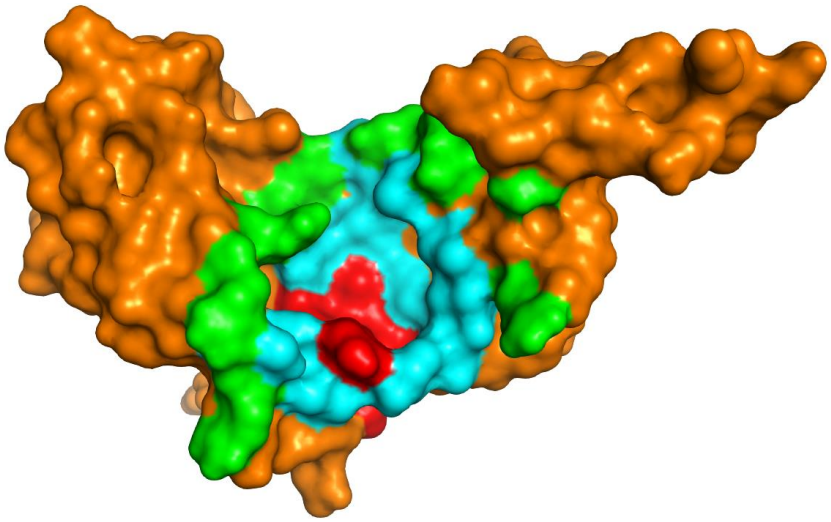

Figure 2. The 3D structure of target protein, HPV 16 E5 protein. Red indicates the main helix structure of the E6 protein, and cyan indicates the E6AP/IRF3 binding pocket, green indicates the E6 pocket residue.

Table 2. Docking and 2D visualization result of top five compounds against HPV16 E6 protein.

Compounds	ΔG	Amino Acid Residue	Interactions (Å)
Asarinin (CID: 11869417) *Zanthoxylum spp* (bark)	-8,2 (kcal/mol)	Cys58; Leu57; Phe52; Ile135; Arg136; Arg138; Ser81; Ser78; Gln114; Val69; Leu74; Val60	Hydrophobic contact
Thiazolo[3,2-a]benzimidazol-3(2H)-one,2-(2-fluorobenzylideno)-7,8-dimethyl (CID: 1823738) *Myristica fragrans* (seeds)	-8.2 (kcal/mol)	Ile135; Arg138; Ser81; Ser78; Val38; Tyr39; Tyr77; Leu74	Hydrophobic contact
Ellagic acid (CID: 5281855) *Syzygium aromaticum* (flowers)	-8.0 (kcal/mol)	Leu57; Gln114; Ser81; Ser78; Tyr77; Leu74; Val69; Phe52	Hydrophobic contact
		Cys58	Hydrophobic contact; Hydrogen bond (2.67); Hydrogen bond (2.99)
		Arg138	Hydrophobic contact; Hydrogen bond (3.03)
Magnoflorine (CID: 73337) *Nigella sativa* (seeds)	-7.9 (kcal/mol)	Ser81; Ile135; Ser78; Tyr77; Arg136; Arg138	Hydrophobic contact
		Gln114	Hydrophobic contact; Hydrogen bond (2.94)
Galbacin (CID: 234441) *Myristica fragrans* (seeds)	-7.8 (kcal/mol)	Leu74; Val69; Tyr39; Val60; Val38; Tyr77; Arg138; Gln114; Ser81	Hydrophobic contact
Vorinostat (CID: 5311) DHAC inhibitor (Drug)	-6.7 (kcal/mol)	Ile135; Arg138; Tyr77; Val69; Thr140; Ser81	Hydrophobic contact
		Gln114	Hydrophobic contact; Hydrogen bond (3.10)
		Ile111	Hydrophobic contact; Hydrogen bond (2.77)
		Ser78	Hydrophobic contact; Hydrogen bond (2.94); Hydrogen bond (2.95)

Mitomycin C (CID: 5746) Anti-cancer drug	-6.4 (kcal/mol)	Leu74; Tyr77; Cys73; Val69; Tyr39; Arg138; Gln114	Hydrophobic contact
		Ser78	Hydrophobic contact; Hydrogen bond (3.13)
		Ser81	Hydrophobic contact; Hydrogen bond (3.16)

Asarinin primarily interacts with the E6AP binding pocket via hydrophobic contacts facilitated by its primary structure. Some key residues involved in the interaction with asarinin include Cys58, Leu57, Arg138, Ser81, Ser78, Gln114, Val69, Leu74, and Val60. It's worth noting that while Arg138 is part of the E6 pocket, Ser78 and Leu74 are also components of the E6 main helix. Additionally, the binding sites of asarinin and both controls exhibit overlap, sharing common residues such as Arg138, Ser81, Ser78, Gln114, Val69, and Leu74.

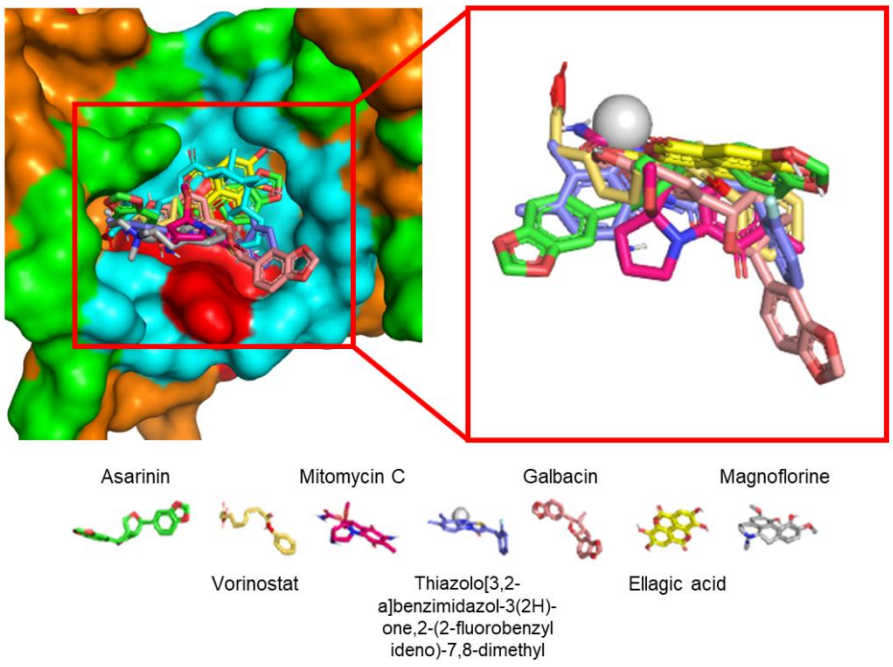

Figure 3. All tested compounds occupied the same binding site. Red indicates the main helix structure of the E6 protein, and cyan indicates the E6AP/IRF3 binding pocket, green indicates the E6 pocket residue.

Thiazolo[3,2-a]benzimidazol-3(2H)-one,2-(2-fluorobenzylideno)-7,8-dimethyl also extensively interacts with the E6AP binding pocket primarily through its primary structure and a hydroxyl group at C7, facilitated by hydrophobic contacts. Critical residues involved in this interaction include Ile135, Arg138, Ser81, Ser78, Tyr39, Tyr77, and Leu75. Notably, while Arg138 is part of the E6 pocket, Ser78 and Leu74 belong to the main helix, and Tyr77 is involved in the E6AP/IRF3 binding pocket, E6 pocket, and the main helix simultaneously. These residues are shared with both drug controls, suggesting a potentially significant role in the compound's mechanism of action.

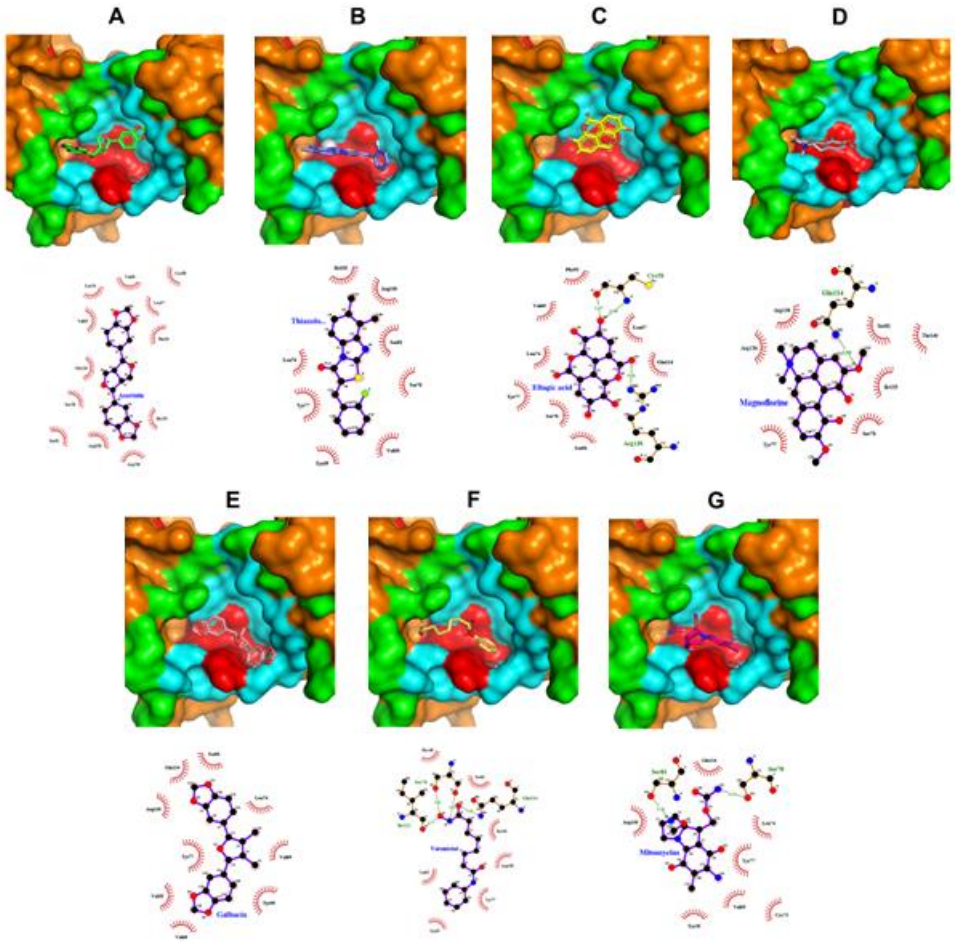

Figure 4. The 3D and 2D structure visualization of binding HPV16 E6 protein and top five compounds molecule (A) asarinin, (B) thiazolo[3,2-a]benzimidazol-3(2H)-one, 2-(2-fluorobenzylideno)-7,8-dimethyl, (C) ellagic acid, (D) magnoflorine, (E) galbacin, (F) vorinostat, and (G) mitomycin C.

Ellagic acid, one of the potential compounds, forms hydrogen bonds with target protein residues. It interacts predominantly with the E6AP/IRF3 binding pocket, overlapping with some E6 pocket and primary helix residues, primarily through its main structure and hydroxyl groups on C11, C5, C7, C13, C12, C6, C8, and C14, facilitated mainly by hydrophobic contacts. Additionally, the hydroxyl groups on C13 and C12 establish moderate to low hydrogen bonds with Cys58 and Arg138, respectively. Critical residues involved in this interaction include Leu57, Gln114, Ser81, Ser78, Tyr77, Leu74, Val69, Cys58, and Arg138, which are commonly shared with the binding sites of vorinostat and mitomycin C.

Similarly, magnoflorine also interacts with the target protein through both hydrophobic contacts and hydrogen bonds. It exhibits nearly identical interactions with the previously mentioned compounds, primarily interacting with the E6AP/IRF3 binding pocket and some overlapping E6 pocket and primary helix residues. Magnoflorine's interactions involve hydrophobic contacts with its main ring structure, methoxy groups on C14 and C17, and a hydroxyl group on C13. The methoxy group on C14 additionally forms a moderate hydrogen bond (2.94Å) with Gln114. Critical residues in this interaction include Ser81, Ile135, Ser78, Tyr77,

Arg136, Arg138, and Gln114, with all except Arg136 being identical to the binding site of the drug controls.

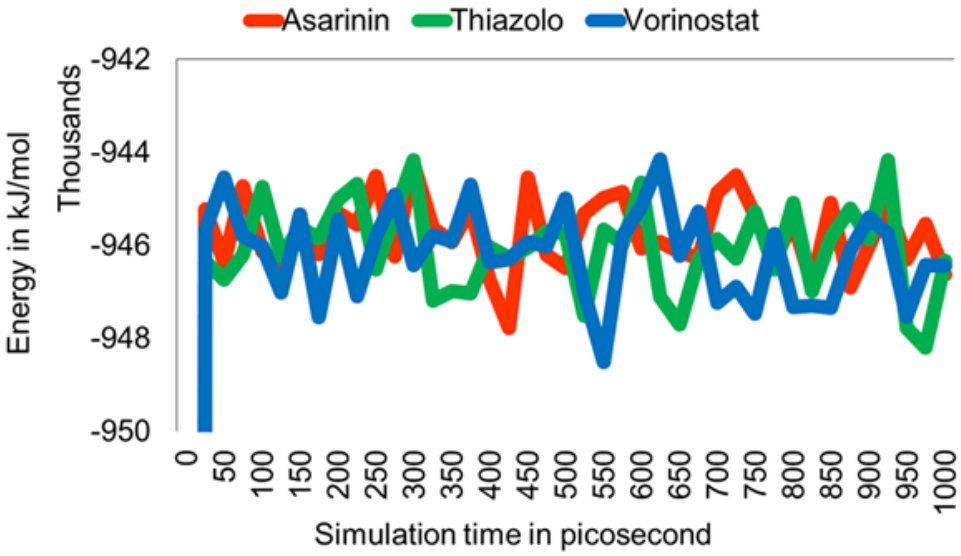

Figure 5. Total potential energy of the system among HPV16 E6 and ligands interaction over a 1000 picosecond simulation.

The last potent compounds in this study, galbacin, predominantly interact with the E6AP/IRF3 binding pocket, along with some overlapping E6 pocket and main helix residues, primarily through hydrophobic contacts, which is consistent with the behavior observed in previous compounds. Notable critical residues involved in this interaction include Leu74, Val69, Tyr39, Val60, Val38, Tyr77, Arg138, Gln114, and Ser81, all of which are identical to the binding site of the drug controls, except for Val60 and Val38.

Regarding the control compounds used in this study, vorinostat and mitomycin C, their interactions with the binding site closely mirror those of the potential compounds. Specifically, vorinostat's binding site residues exhibit a similarity of approximately 77% with the residues interacting with the rest of the potential compounds from various natural sources. Similarly, mitomycin C's binding site interactions are nearly 88% identical to those of the top five compounds. Both controls share about 67% of their binding site residues, including some highly conserved residues such as Arg138, Tyr77, Ser81, and Gln114.

Based on the docking and visualization results, we selected the top two compounds and vorinostat as a control for further analysis using molecular dynamics. Essential parameters such as potential energy, RMSD, and RMSF values were monitored over 1000 picoseconds of simulation to provide insights into the dynamic behavior of the protein-ligand complexes.

The root mean square deviation (RMSD) was computed utilizing 1000 picoseconds of simulation to evaluate the flexibility and overall stability of the docked complexes (Fig. 6). The RMSD value for E6-asarinin was 4.163±0.758Å, with a minimum of 0.600Å and a maximum of 5.151Å. The E6-thiazolo[3,2-a]benzoidazole-3(2H)-one,2-(2fluorobenzylideno)-7,8-dimethyl complex has a mean value of 3.641±1.203Å, ranging from 0.600 to 5.594Å. The mean value of E6-vorinostat was 6.206±1.484Å, with a minimum value of 0.591Å and a maximum value of 7.999Å.

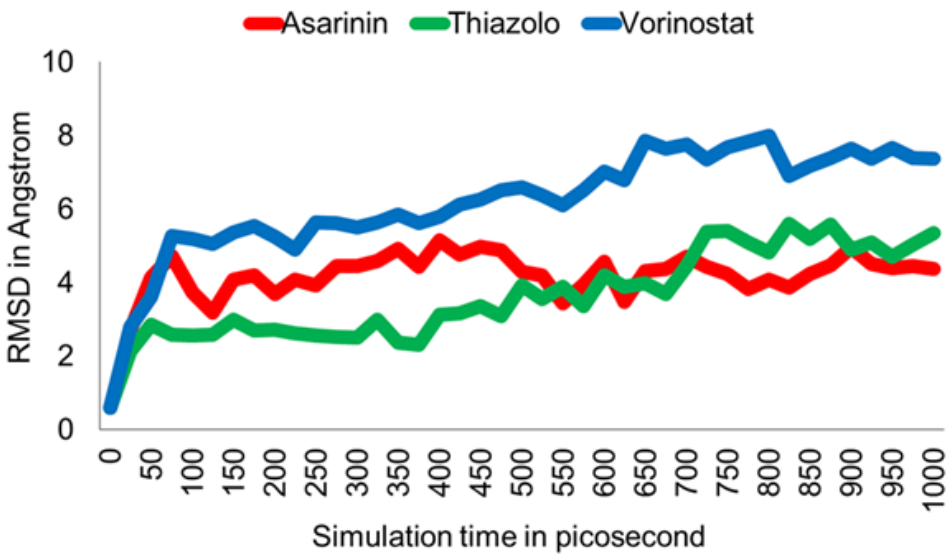

Figure 6. RMSD plot for HPV16 E6 and Asarinin (red line), Thiazolo (green line), and Vorinostat (blue line) complexes over a 1000 picosecond of simulation.

The RMSD plot illustrates that both candidate compounds exhibit significantly lower RMSD values compared to the controls. In the case of the asarinin complex, after initial oscillations between 0 and 150 ps, it stabilizes around 4. On the other hand, the thiazolo[3,2-a]benzoidazole-3(2H)-one,2-(2-fluorobenzylideno)-7,8-dimethyl complex demonstrates stability between 50 and 400 ps, maintaining an RMSD around 3 before showing a slight increase in values towards the end of the simulation, ranging from 5 to 5.5. In contrast, the vorinostat complex exhibits a continuous increase in RMSD values throughout the simulation period.

Based on the trajectory graph, it appears that the E6-asarinin complex is the most stable protein-ligand combination, followed by the thiazolo[3,2-a]benzoidazole-3(2H)-one,2-(2-fluorobenzylideno)-7,8-dimethyl complex, which remains stable up to 400 ps before displaying a slight increase in RMSD values. Meanwhile, the vorinostat complex exhibits a steady rise in RMSD values throughout the simulation, indicating potential instability in the protein-ligand interaction over time.

The RMSF plot (Fig. 7) highlights that, aside from the N- and C-termini, there were minimal variations observed across the residues for both potential compounds throughout the simulation period. This indicates a well-organized synthesis of these two protein-ligand complexes. In contrast, the vorinostat complex consistently exhibited higher RMSF values and more significant oscillations compared to the other two compounds investigated, suggesting that vorinostat was the least stable among the three substances during the molecular dynamics simulation. However, it's worth noting that all compounds displayed low RMSF values for the residues with which they interacted, indicating relatively stable interactions despite differences in overall stability.

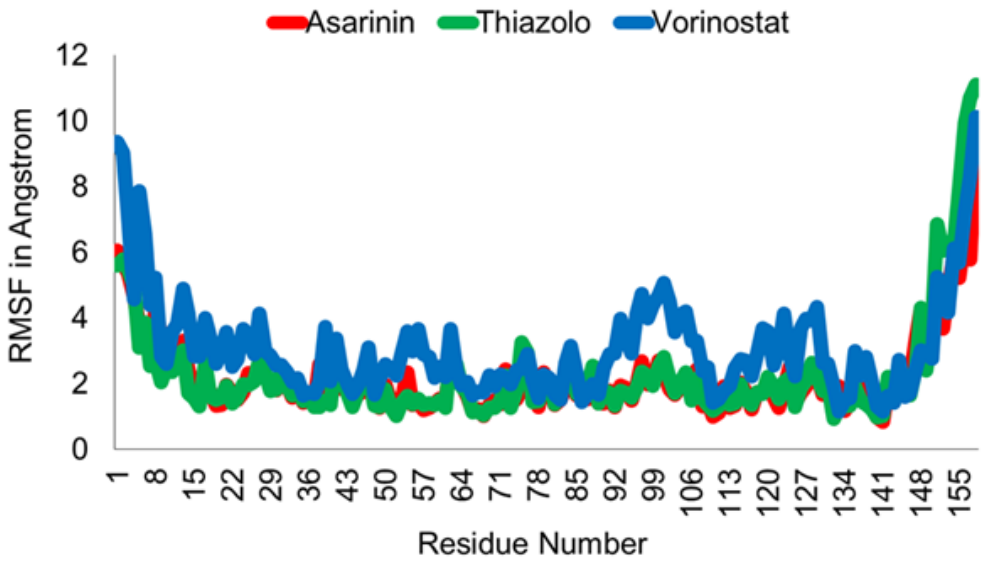

Figure 7. RMSF plot for HPV16 E6 and Asarinin (red line), Thiazolo (green line), and Vorinostat (blue line) complexes residues over a 1000 picosecond simulation.

DISCUSSION

One of the crucial roles of E6 protein in cervical cancer development is the degradation of p53, which stimulates cell proliferation and prevents apoptosis, also the degradation of DLG1 or NFX1 hosts, which will lead to upregulation of human telomerase reverse transcriptase (hTERT), and ends in cell immortalization (Bernard et al. 2011; Doorbar et al. 2012; Sekaric et al. 2008; Van Doorslaer & Burk 2010). However, to carry out these functions, the E6 protein cannot stand alone but formed a complex with E6AP (Martinez-Zapien et al. 2016; Sailer et al. 2018). E6, E6AP, and p53 complexes already visualized by PDB entry ID 4XR8 (Martinez-Zapien et al. 2016). The E6-E6AP complex is connected through a helix linker structure known as leucine (L)-rich motifs (LxxLL), which binds to residues around the E6 protein main alpha helix, the main target in this study. The disruption between E6 protein and E6AP is predicted to inhibit the E6-E6AP complex formation, lowering the degradation rate of p53. In this experiment, the disturbance was carried out with potent natural compounds expected to occupy the same binding site as E6AP to act as a competitive inhibitor. A similar interaction mechanism also occurs in the formation of the E6-IRF3 complex. Interestingly, the E6-IRF3 complex connected by the interaction between IRF3's LxxLL motif and the hydrophobic pocket E6 protein around its main alpha helix (Reiser et al. 2011; Ronco et al. 1998; M. Shah et al. 2013). Thus, the E6-E6AP complex formation disturbance by some potential compounds were expecting acting as a competitive inhibitor at the E6AP binding site.Furthermore, we hypothesized that the interference also occurs in the E6-IRF3 complex due to the LxxLL motifs formation, since the E6AP and IRF3 have identical binding sites.

The docking results showed that all of the top five compounds had lower affinity values than the two-drug controls, indicates that the interaction between the top five compounds with the target protein is more stable than the interaction between the controls and the target protein (Pantsar & Poso 2018; Trott & Olson 2009), and have higher tendency to form interactions between top five compounds and target protein than drug controls (Murcko & Ajay 1995). The asarinin found in *Zanthoxylum spp* and thiazolo[3,2-a]benzimidazol-3(2H)-one,2-(2-fluorobenzylideno)-7,8-dimethyl found in *Myristica fragrans* are two potential compounds that have the best affinity values based on docking result. Their lowest affinity is 8.2 kcal/mol, roughly

22.3% and 28% lower than vorinostat and mitomycin C, respectively. Thus, these tend to form a more stable interaction with the E6AP/IRF3 binding pocket on the E6 protein than the rest of the natural compounds and drug controls. However, asarinin interacts with more E6AP/IRF3 binding pocket residues than thiazolo[3,2-a]benzimidazole-3(2H)-one,2-(2-fluorobenzylideno)-7,8-dimethyl (10 to 8 residues), Although the difference in the number of interactions is not significant, it is suspected that there is an effect on the stability of the interactions formed between each compound and the E6AP/IRF3 binding pocket. All interactions established between the two compounds and the E6AP/IRF3 binding pocket are characterized as hydrophobic interactions, which are inherently stronger at a molecular level compared to other intermolecular interactions such as hydrogen bonds or Van der Waals bonds (Atkins & Paula 2010; Jeffrey 1997).

The two top-five compounds that form simultaneous hydrophobic interactions and hydrogen bonds are ellagic acid found in *Syzygium aromaticum* and magnoflorine found in *Nigella sativa*. The two compounds were also known to have better affinity values than the controls. The docking results show that the hydrogen bonds formed in the two compounds are moderate, primarily electrostatic, and act as supporting bonds because they have a donor-acceptor distance in the 2.5-3.2Å range, and as a whole, these compounds do not have better affinity than asarinin, which entirely relies on hydrophobic contacts (Jeffrey 1997).

The top five compounds and the two drug controls have binding sites on the E6 protein almost identical to each other, characterized by several conserved residues mentioned above; only three residues (4.7%) that exclusively interact with one compound, including Cys73, Ile111, and Thr140. The visualization results in Fig. 2 confirmed the 2D visualization results even further. The stable interaction between the top five compounds at the E6AP's LxxLL motif binding site is predicted to inhibit the formation of the E6-E6AP complex that is crucial in the p53 degradation process by preventing the E6AP's LxxLL domain from binding to its specific binding site. The interaction between E6AP's LxxLL motif and E6 protein will trigger a conformational change of the E6 protein into a suitable and stable conformation to bind with p53, characterized by the formation of the p53 binding cleft (Sailer et al. 2018; Vande Pol & Klingelhutz 2013), inhibiting the degradation process of p53 because E6 and E6AP are not stable enough to be carried out the p53 binding and degradation process itself. It is predicted that the mechanism of action of p53 can still manageably running, mainly causing cells infection to apoptosis (Huibregtse et al. 1993; Martinez-Zapien et al. 2016).

In addition, the top five compounds' interaction is also thought to affect the formation of the E6-IRF3 complex because the IRF3's LxxLL motifs have a binding site that is identical to the LxxLL motif possessed by E6AP (M. Shah et al. 2013). The stable form of the E6-IRF3 complex is found exclusively in the HPV16 variant. The binding of the IRF3's LxxLL motif to the E6 protein does not cause IRF3 degradation; instead, it suppresses the transactivation process, which will inhibit IFN-β transcription (Westrich et al. 2017). IRF3 has 2 LxxLL motifs in its N-terminal (140-LDELLG-145 (IRF3-LR1) and 192-LKRLLV-197 (IRF3-LR2)), and autoinhibitory domain (AD) that flank the IRF association domain (IAD) in its C-terminal (Chen & Royer 2010; R. Lin et al. 1999). When the E6 protein binds to IRF3 through its LxxLL motif, the E6 protein will change its conformation to interact with Ser-patches on IRF3. The interaction of E6 protein with Ser-patches on IRF3 will inhibit the activation process of IRF3 through a phosphorylation mechanism so that there is no co-activation process of IFN-β transcription with p300/CBP (Howie et al. 2009; M. Shah et al. 2013). In addition, the interaction between E6 and IRF3 will result in the phosphorylation of the AD domain by virus-induced kinase, thus keeping IRF3 in an inactivated state (Tummers & van der Burg 2015). Therefore, the disruption of E6-IRF3 complex formation by some potential compounds is thought to undisturbed signaling mechanism and activation of

the IRF3 pathway so that the overall innate immune response performs better against HPV16 infection.

To deepen the analysis, we performing molecular dynamic simulation as our previous study (Hidayatullah et al. 2022). Asarinin and thiazolo[3,2-a]benzoidazole-3(2H)-one,2-(2-fluorobenzylideno)-7,8-dimethyl, the two of the top compounds, have relatively lower RMSD and RMSF values than the control, indicating that the complex formed by the two compounds is more stable than vorinostat used as a control. The RMSF plot shows consistent low values for residues suspected to interact with these two compounds and control based on the results of 2D visualization, indicating that these residues are critical in the active site of the HPV16 E6 protein's hydrophobic groove and indicate stability in the residue region bound to the tested ligands (Aier et al. 2016; Zhao et al. 2015).

CONCLUSION

The majority of cervical cancer cases are attributed to HPV16 infection, with the E6 protein serving as a key oncoprotein implicated in cancer development. Docking and visualization results reveal that all of the top five compounds are concentrated within a single binding site on the E6 main hydrophobic groove, which coincides with the binding site of the E6AP and IRF3's LxxLL motifs. These compounds are predicted to function as competitive inhibitors, potentially obstructing the formation of the E6-E6AP and E6-IRF3 complexes. By doing so, they may hinder the degradation of p53, consequently impeding cell proliferation, and sustaining the innate immune response against HPV16 infection. Notably, asarinin and thiazolo[3,2-a]benzimidazole-3(2H)-one,2-(2-fluorobenzylideno)-7,8-dimethyl emerged as the most potent compounds, exhibiting the highest affinity value (-8.2 kcal/mol) and forming stable interactions with the E6 main hydrophobic groove. However, further investigations utilizing in vivo or in vitro methods are warranted to validate the computational predictions presented in this study.

ACKNOWLEDGEMENTS

Authors thank Universitas Negeri Malang for provided research instruments. We declare that there was no funding received for this study.

AUTHORS' CONTRIBUTIONS

This study has had an equal contribution from all authors. Finally, authors evaluated and approved the final version of manuscript for publication.

REFERENCES

Abdallah E, Elsharkawy E and Ed-Dra A. (2016). Biological activities of methanolic leaf extract of *Ziziphus mauritiana*. *Bioscience Biotechnology Research Communications 9*: 605–614. https://doi.org/10.21786/bbrc/9.4/6

Abdel-Moneim A, Morsy B M, Mahmoud A M, Abo-Seif M A and Zanaty M I. (2013). Beneficial therapeutic effects of *Nigella sativa* and/or *Zingiber officinale* in HCV patients in Egypt. *EXCLI Journal 12*: 943–955.

Aier I, Varadwaj P K and Raj U. (2016). Structural insights into conformational stability of both wild-type and mutant EZH2 receptor. *Scientific Reports 6*(1): 1–10. https://doi.org/10.1038/srep34984

Amalina A N, Natanamurugaraj G, Mashitah M Y and Nurul A A K. (2013). Chemical composition, antioxidant and antibacterial activities of syzygium polyanthum (Wight) Walp. essential oils. *The Open Conference Proceedings Journal 4*(1): 139. http://dx.doi.org/10.2174/2210289201304010139

Anwar F, Ali M, Hussain A I and Shahid M. (2009). Antioxidant and antimicrobial activities of essential oil and extracts of fennel (*Foeniculum vulgare* Mill.) seeds from Pakistan. *Flavour and Fragrance Journal 24*(4): 170–176. https://doi.org/10.1002/ffj.1929

Arbyn M, Weiderpass E, Bruni L, Sanjosé S de, Saraiya M, Ferlay J and Bray F. (2020). Estimates of incidence and mortality of cervical cancer in 2018: A worldwide analysis. *The Lancet Global Health 8*(2): 191–203. https://doi.org/10.1016/S2214-109X(19)30482-6

Asika A O, Adeyemi O T, Anyasor G N, Gisarin O and Osilesi O. (2016). GC-MS Determination of bioactive compounds and nutrient composition of *Myristica fragrans* Seeds. *Journal of Herbs, Spices & Medicinal Plants 22*(4): 337–347. https://doi.org/10.1080/10496475.2016.1223248

Atkins P and Paula J de. (2010). *Physical Chemistry for the Life Sciences* (Second Edition). Oxford University Press.

Badgujar S B, Patel V V and Bandivdekar A H. (2014). *Foeniculum vulgare* Mill: A Review of Its Botany, Phytochemistry, Pharmacology, Contemporary Application, and Toxicology. *BioMed Research International 2014*: 1–32. https://doi.org/10.1155/2014/842674

Banerjee N S, Moore D W, Broker T R and Chow L T. (2018). Vorinostat, a pan-HDAC inhibitor, abrogates productive HPV-18 DNA amplification. *Proceedings of the National Academy of Sciences of the United States of America 115*(47): E11138–E11147. https://doi.org/10.1073/pnas.1801156115

Beers S J. (2012). *Jamu: The ancient Indonesian art of herbal healing*. Tuttle Publishing.

Bernard X, Robinson P, Nominé Y, Masson M, Charbonnier S, Ramirez-Ramos J R, Deryckere F, Travé G and Orfanoudakis G. (2011). Proteasomal degradation of p53 by human papillomavirus E6 oncoprotein relies on the structural integrity of p53 core domain. *PloS One 6*(10): 1–10. https://doi.org/10.1371/journal.pone.0025981

Beyzi E, Karaman K, Gunes A and Buyukkilic Beyzi S. (2017). Change in some biochemical and bioactive properties and essential oil composition of coriander seed (Coriandrum sativum L.) varieties from Turkey. *Industrial Crops and Products 109*: 74–78. https://doi.org/10.1016/j.indcrop.2017.08.008

Bonnez W. (2009). Chapter 26—Human Papillomavirus. In A D T Barrett and L R Stanberry (Eds.), *Vaccines for Biodefense and Emerging and Neglected Diseases* (pp. 469–496). Academic Press. https://doi.org/10.1016/B978-0-12-369408-9.00026-3

Bzhalava D, Guan P, Franceschi S, Dillner J and Clifford G. (2013). A systematic review of the prevalence of mucosal and cutaneous human papillomavirus types. *Virology 445*(1): 224–231. https://doi.org/10.1016/j.virol.2013.07.015

Chen W and Royer W E. (2010). Structural insights into interferon regulatory factor activation. *Cellular Signalling 22*(6): 883–887. https://doi.org/10.1016/j.cellsig.2009.12.005

Choi O, Cho S K, Kim J, Park C G and Kim J. (2016). In vitro antibacterial activity and major bioactive components of Cinnamomum verum essential oils against cariogenic bacteria, *Streptococcus mutans* and *Streptococcus sobrinus*. *Asian Pacific Journal of Tropical Biomedicine 6*(4): 308–314. https://doi.org/10.1016/j.apjtb.2016.01.007

Chung H -J. (2009). Evaluation of the biological activity of extracts from star-anise (*Illicium verum*). *Preventive Nutrition and Food Science 14*(3): 195–200. https://doi.org/10.3746/jfn.2009.14.3.195

Cobo F. (2012). 1—Introduction and epidemiological data. In F Cobo (Ed.), *Human Papillomavirus Infections* (pp. 1–14). Woodhead Publishing. https://doi.org/10.1533/9781908818171.1

Dilla Dertyasasa E and Anindito Sri Tunjung W. (2017). Volatile organic compounds of kaffir lime (*Citrus hystrix* DC.) leaves fractions and their potency as traditional medicine. *Biosciences, Biotechnology Research Asia 14*(4): 1235–1250. https://doi.org/10.13005/bbra/2566

Doorbar J, Quint W, Banks L, Bravo I G, Stoler M, Broker T R and Stanley M A. (2012). The biology and life-cycle of human papillomaviruses. *Vaccine 30*: 55–70. https://doi.org/10.1016/j.vaccine.2012.06.083

Egawa N and Doorbar J. (2017). The low-risk papillomaviruses. *Virus Research 231*: 119–127. https://doi.org/10.1016/j.virusres.2016.12.017

Ekpenyong C E, Akpan E and Nyoh A. (2015). Ethnopharmacology, phytochemistry, and biological activities of *Cymbopogon citratus* (DC.) Stapf extracts. *Chinese Journal of Natural Medicines 13*(5): 321–337. https://doi.org/10.1016/S1875-5364(15)30023-6

El-Saber Batiha G, Alkazmi L M, Wasef L G, Beshbishy A M, Nadwa E H and Rashwan E K. (2020). *Syzygium aromaticum* L. (Myrtaceae): Traditional uses, bioactive chemical constituents, pharmacological and toxicological activities. *Biomolecules 10*(2): 202. https://doi.org/10.3390/biom10020202

Fagodia S K, Singh H P, Batish D R and Kohli, R. K. (2017). Phytotoxicity and cytotoxicity of *Citrus aurantiifolia* essential oil and its major constituents: Limonene and citral. *Industrial Crops and Products 108*: 708–715. https://doi.org/10.1016/j.indcrop.2017.07.005

Figueirinha A, Paranhos A, Pérez-Alonso J J, Santos-Buelga C and Batista M T. (2008). *Cymbopogon citratus* leaves: Characterization of flavonoids by HPLC–PDA–ESI/MS/MS and an approach to their potential as a source of bioactive polyphenols. *Food Chemistry 110*(3): 718–728.

Forcier M and Musacchio N. (2010). An overview of human papillomavirus infection for the dermatologist: Disease, diagnosis, management, and prevention. *Dermatologic Therapy 23*(5): 458–476. https://doi.org/10.1111/j.1529-8019.2010.01350.x

González-Molina E, Domínguez-Perles R, Moreno D A and García-Viguera C. (2010). Natural bioactive compounds of *Citrus limon* for food and health. *Journal of Pharmaceutical and Biomedical Analysis 51*(2): 327–345. https://doi.org/10.1016/j.jpba.2009.07.027

Graham S V. (2017). The human papillomavirus replication cycle, and its links to cancer progression: A comprehensive review. *Clinical Science 131*(17): 2201–2221. https://doi.org/10.1042/CS20160786

Gutiérrez-Hoya A and Soto-Cruz I. (2020). Role of the JAK/STAT Pathway in cervical cancer: Its relationship with HPV E6/E7 oncoproteins. *Cells 9*(10): 2297. https://doi.org/10.3390/cells9102297

Hakim L. (2015). *Rempah dan herba kebun pekarangan rumah masyarakat: keragaman, sumber fitofarmaka dan wisata kesehatan-kebugaran*. Diandra Creative, Indonesia.

Hidayatullah A, Putra W E, Rifa'i M, Sustiprijatno, Widiastuti D, Heikal M F, Susanto H, Salma O. (2022). Molecular docking and dynamics simulation studies to predict multiple medicinal plants' bioactive compounds interaction and its behavior on the surface of DENV-2 E protein. *Karbala International Journal of Modern Science 8*(3): 531-542. https://doi.org/10.33640/2405-609X.3237

Hidayatullah A, Putra W E, Salma W O, Muchtaromah B, Permatasari G W, Susanto H, Widiastuti D and Kismurtono M. (2020). Discovery of drug candidate from various

natural products as potential novel dengue virus nonstructural protein 5 (NS5) inhibitor. *Chiang Mai University Journal of Natural Sciences 20*(1): 1-17. https://doi.org/10.12982/CMUJNS.2021.018

Hidayatullah A, Putra W E, Sustiprijatno, Permatasari G W, Salma W O, Widiastuti D, Susanto H, Muchtaromah B, Sari D R T, Ningsih F N, Heikal M F, Yusuf A M R and Arizona A S. (2021). In silico targeting DENV2's prefusion envelope protein by several natural products' bioactive compounds. *Chiang Mai University Journal of Natural Sciences 20*(3): 1-20. https://doi.org/10.12982/CMUJNS.2021.059

Hidayatullah A, Putra W E, Sustiprijatno, Widiastuti D, Salma W O and Heikal M F. (2023). Molecular docking and molecular dynamics simulation-based identification of natural inhibitors against druggable human papilloma virus type 16 target. *Trends in Sciences 20*(4): 1-12. https://doi.org/10.48048/tis.2023.4891

Howie H L, Katzenellenbogen R A and Galloway D A. (2009). Papillomavirus E6 proteins. *Virology 384*(2): 324–334. https://doi.org/10.1016/j.virol.2008.11.017

Huibregtse J M, Scheffner M and Howley P M. (1993). Localization of the E6-AP regions that direct human papillomavirus E6 binding, association with p53, and ubiquitination of associated proteins. *Molecular and Cellular Biology 13*(8): 4918–4927. https://doi.org/10.1128/MCB.13.8.4918

Jayaram B, Singh T, Mukherjee G, Mathur A, Shekhar S and Shekhar V. (2012). Sanjeevini: A freely accessible web-server for target directed lead molecule discovery. *BMC Bioinformatics 13*(17): 1–13. https://doi.org/10.1186/1471-2105-13-S17-S7

Jeffrey G A. (1997). *An introduction to hydrogen bonding*. Oxford University Press.

Jennifer H and Saptutyningsih E. (2015). Preferensi individu terhadap pengobatan tradisional di Indonesia. *Jurnal Ekonomi dan Studi Pembangunan 16*(1): 16.

Kadam D and Lele S S. (2017). Extraction, characterization and bioactive properties of Nigella sativa seedcake. *Journal of Food Science and Technology 54*(12): 3936–3947. https://doi.org/10.1007/s13197-017-2853-8

Kang Y H, Lee K -A, Kim J -H, Park S -G and Yoon D -Y. (2010). Mitomycin C modulates DNA-double strand break repair genes in cervical carcinoma cells. *Amino Acids 39*(5): 1291–1298. https://doi.org/10.1007/s00726-010-0568-5

Kitchen D B, Decornez H, Furr J R and Bajorath J. (2004). Docking and scoring in virtual screening for drug discovery: Methods and applications. *Nature Reviews Drug Discovery 3*(11): Article 11. https://doi.org/10.1038/nrd1549

Kristianto S, Batoro J, Widyarti S and Sumitro S. (2020, October 31). *Exploration and Economic Value of Medicinal Plants as Traditional Herbal Ingredients in Bangselok, Madura, Indonesia*.

Laribi B, Kouki K, M'Hamdi M and Bettaieb T. (2015). Coriander (Coriandrum sativum L.) and its bioactive constituents. *Fitoterapia 103*: 9–26. https://doi.org/10.1016/j.fitote.2015.03.012

Li S -G, Zhou B -G, Li M -Y, Liu S, Hua R -M and Lin H -F. (2017). Chemical composition of Illicium verum fruit extract and its bioactivity against the peach–potato aphid, *Myzus persicae* (Sulzer). *Arthropod-Plant Interactions 11*(2): 203–212. https://doi.org/10.1007/s11829-016-9480-6

Lin R, Mamane Y and Hiscott J. (1999). Structural and functional analysis of interferon regulatory factor 3: Localization of the transactivation and autoinhibitory domains. *Molecular and Cellular Biology 19*(4): 2465–2474.

Lin Z, Bazzaro M, Wang M -C, Chan K, Peng S and Roden R. (2009). Combination of proteasome and HDAC inhibitors for uterine cervical cancer treatment. *Clinical Cancer Research 15*: 570–577. https://doi.org/10.1158/1078-0432.CCR-08-1813

Lionta E, Spyrou G K, Vassilatis D and Cournia Z. (2014). Structure-based virtual screening for drug discovery: Principles, applications and recent advances. *Current Topics in Medicinal Chemistry 14*(16): 1923–1938.

Mahmood M S, Mártinez J L, Aslam A, Rafique A, Vinet R, Laurido C, Hussain I, Abbas R Z, Khan A and Ali S. (2016). Antiviral effects of green tea (*Camellia sinensis*) against pathogenic viruses in human and animals (a mini-review). *African Journal of Traditional, Complementary and Alternative Medicines 13*(2): 176. https://doi.org/10.4314/ajtcam.v13i2.21

Majdi C, Pereira C, Dias M I, Calhelha R C, Alves M J, Rhourri-Frih B, Charrouf Z, Barros L, Amaral J S and Ferreira I C F R. (2020). Phytochemical characterization and bioactive properties of cinnamon basil (*Ocimum basilicum* cv. 'Cinnamon') and Lemon Basil (*Ocimum* × *citriodorum*). *Antioxidants 9*(5): 369. https://doi.org/10.3390/antiox9050369

Martinez-Zapien D, Ruiz F X, Poirson J, Mitschler A, Ramirez J, Forster A, Cousido-Siah A, Masson M, Pol S V, Podjarny A, Travé G and Zanier K. (2016). Structure of the E6/E6AP/p53 complex required for HPV-mediated degradation of p53. *Nature 529*(7587): 541–545. https://doi.org/10.1038/nature16481

Mirzaei H, Zarbafian S, Villar E, Mottarella S, Beglov D, Vajda S, Paschalidis I Ch, Vakili P and Kozakov D. (2015). Energy minimization on manifolds for docking flexible molecules. *Journal of Chemical Theory and Computation 11*(3): 1063–1076. https://doi.org/10.1021/ct500155t

Mohammed, Y. H., Ghaidaa, J. M and Imad, H. H. (2016). Analysis of bioactive chemical compounds of Nigella sativa using gas chromatography-mass spectrometry. *Journal of Pharmacognosy and Phytotherapy 8*(2): 8–24. https://doi.org/10.5897/JPP2015.0364

Murcko M A and Ajay. (1995). Computational methods to predict binding free energy in ligand-receptor complexes. *Journal of Medicinal Chemistry 38*(26): 4953–4967. https://doi.org/10.1021/jm00026a001

Pandey R, Mahar R, Hasanain M, Shukla S K, Sarkar J, Rameshkumar K B and Kumar B. (2016). Rapid screening and quantitative determination of bioactive compounds from fruit extracts of Myristica species and their in vitro antiproliferative activity. *Food Chemistry 211*: 483–493. https://doi.org/10.1016/j.foodchem.2016.05.065

Pantsar T and Poso A. (2018). Binding Affinity via Docking: Fact and fiction. *Molecules : A Journal of Synthetic Chemistry and Natural Product Chemistry 23*(8). https://doi.org/10.3390/molecules23081899

Patil J R, Chidambara Murthy K N, Jayaprakasha G K, Chetti M B and Patil B S. (2009). Bioactive compounds from Mexican lime (*Citrus aurantifolia*) juice induce apoptosis in human pancreatic cells. *Journal of Agricultural and Food Chemistry 57*(22): 10933–10942. https://doi.org/10.1021/jf901718u

Patra J K, Das G, Bose S, Banerjee S, Vishnuprasad C N, Pilar Rodriguez-Torres M and Shin H. (2020). Star anise (*Illicium verum*): Chemical compounds, antiviral properties, and clinical relevance. *Phytotherapy Research 34*(6): 1248–1267. https://doi.org/10.1002/ptr.6614

Piras A, Rosa A, Marongiu B, Porcedda S, Falconieri D, Dessì M A, Ozcelik B and Koca U. (2013). Chemical composition and in vitro bioactivity of the volatile and fixed oils of

Nigella sativa L. extracted by supercritical carbon dioxide. *Industrial Crops and Products 46*: 317–323. https://doi.org/10.1016/j.indcrop.2013.02.013

Putra W E and Rifa'i M. (2020). Evaluating the molecular interaction of Sambucus plant bioactive compounds toward TNF-R1 and TRAIL-R1/R2 as possible anti-cancer therapy based on traditional medicine: The bioinformatics Study. *Scientific Study & Research - Chemistry & Chemical Engineering, Biotechnology, Food Industry 21*(3): 357-365.

Putra W E. (2018). In silico study demonstrates multiple bioactive compounds of sambucus plant promote death cell signaling pathway via fas receptor. *FUW Trends in Science & Technology Journal 3*(2): 682-685.

Putra W E, Salma W O and Rifa'i M. (2019). Anti-inflammatory activity of Sambucus plant bioactive compounds against TNF-α and TRAIL as solution to overcome inflammation associated diseases: The insight from bioinformatics study. *Natural Product Sciences 25*(3): 215-221. https://doi.org/10.20307/nps.2019.25.3.215

Putra W E, Salma W O and Widiastuti D. (2021). Computational investigation of isorhamnetin-3, quercetin-3, and quercetin from *Alstonia scholaris* as the potential anti-inflammatory agents against Cox-2*. Malaysian Journal of Biochemistry & Molecular Biology 24*(2): 106-109.

Putra W E, Salma W O, Widiastuti D and Kismurtono M. (2020). In silico screening of peroxisome proliferator activated receptor gamma (PPARG)-agonist from *Eugenia jambolana* bioactive compounds as potential anti-diabetic agent. *Malaysian Journal of Biochemistry & Molecular Biology 23*(2): 142-146.

Putra W E, Sustiprijatno, Hidayatullah A, Heikal M F, Widiastuti D and Isnanto H. (2023). Analysis of three non-structural proteins, Nsp1, Nsp2, and Nsp10 of Sars-Cov-2 as pivotal target proteins for computational drug screening. *Journal of Microbiology, Biotechnology and Food Sciences 12*(5): 1-6. https://doi.org/10.55251/jmbfs.9586

Putra W E, Waffareta E, Ardiana O, Januarisasi I D, Soewondo A and Rifa'i M. (2017). Dexamethasone-administrated BALB/c mouse promotes proinflammatory cytokine expression and reduces $CD4^{+}CD25^{+}$ regulatory T cells population. *Bioscience Research 14*(2): 201-213.

Putri A R, Khaerunnisa S and Yuliati I. (2019). Cervical cancer risk factors association in patients at the gynecologic-oncology clinic of Dr. Soetomo Hospital Surabaya. *Indonesian Journal of Cancer 13*(4): 104. https://doi.org/10.33371/ijoc.v13i4.610

Rattanachaikunsopon P and Phumkhachorn P. (2010). Potential of cinnamon (*Cinnamomum verum*) oil to control Streptococcus iniae infection in tilapia (*Oreochromis niloticus*). *Fisheries Science 76*(2): 287–293. https://doi.org/10.1007/s12562-010-0218-6

Reiser J, Hurst J, Voges M, Krauss P, Münch P, Iftner T and Stubenrauch F. (2011). High-Risk human papillomaviruses repress constitutive kappa interferon transcription via E6 to prevent pathogen recognition receptor and antiviral-gene expression. *Journal of Virology 85*(21): 11372–11380. https://doi.org/10.1128/JVI.05279-11

Ricci-López J, Vidal-Limon A, Zunñiga M, Jimènez V A, Alderete J B, Brizuela C A and Aguila S. (2019). Molecular modeling simulation studies reveal new potential inhibitors against HPV E6 protein. *PloS One 14*(3): 1–22. https://doi.org/10.1371/journal.pone.0213028

Rietz A, Petrov D, Bartolowits M, DeSmet M, Davisson V and Androphy E. (2016). Molecular probing of the HPV-16 E6 protein alpha helix binding groove with small molecule inhibitors. *PloS One 11*: 1–20. https://doi.org/10.1371/journal.pone.0149845

Ronco L V, Karpova A Y, Vidal M and Howley P M. (1998). Human papillomavirus 16 E6 oncoprotein binds to interferon regulatory factor-3 and inhibits its transcriptional activity. *Genes & Development 12*(13): 2061–2072. https://doi.org/10.1101/gad.12.13.2061

Tan S, de Vries E G, van der Zee A G and de Jong S. (2012). Anticancer drugs aimed at E6 and E7 activity in HPV-positive cervical cancer. *Current Cancer Drug Targets 12*(2): 170–184.

Sailer C, Offensperger F, Julier A, Kammer K -M, Walker-Gray R, Gold M G, Scheffner M and Stengel F. (2018). Structural dynamics of the E6AP/UBE3A-E6-p53 enzyme-substrate complex. *Nature Communications 9*: 1–12. https://doi.org/10.1038/s41467-018-06953-0

Salim Z and Munadi E. (2017). *Info Komoditi Tanaman Obat*. Badan Pengkajian dan Pengembangan Perdagangan Kementerian Perdagangan Republik Indonesia.

Scheurer M E, Tortolero-Luna G and Adler-Storthz K. (2005). Human papillomavirus infection: Biology, epidemiology, and prevention. *International Journal of Gynecological Cancer 15*(5): 727–746. https://doi.org/10.1111/j.1525-1438.2005.00246.x

Sekaric P, Cherry J J and Androphy E J. (2008). Binding of human papillomavirus type 16 E6 to E6AP is not required for activation of hTERT. *Journal of Virology 82*(1): 71–76. https://doi.org/10.1128/JVI.01776-07

Shah G, Shri R, Panchal V, Sharma N, Singh B and Mann A S. (2011). Scientific basis for the therapeutic use of *Cymbopogon citratus*, stapf (Lemon grass). *Journal of Advanced Pharmaceutical Technology & Research 2*(1): 3.

Shah M, Wadood A, Rahman Z and Husnain T. (2013). Interaction and inhibition of dengue envelope glycoprotein with mammalian receptor DC-Sign, an In-silico approach. *PloS One 8*(3): 1–10. https://doi.org/10.1371/journal.pone.0059211

Srivastava A K, Srivastava S K and Syamsundar K V. (2005). Bud and leaf essential oil composition of Syzygium aromaticum from India and Madagascar. *Flavour and Fragrance Journal 20*(1): 51–53. https://doi.org/10.1002/ffj.1364

Sukandar D, Hermanto S, Amelia E R and Zaenudin M. (2016). Aktivitas antibakteri ekstrak biji kapulaga (*Amomum compactum* Sol. Ex Maton). *Jurnal Kimia Terapan Indonesia 17*(2): 119–129. https://doi.org/10.14203/jkti.v17i2.28

Sumayyah S and Salsabila N. (2017). Obat tradisional: Antara khasiat dan efek sampingnya. *Majalah Farmasetika 2*(5): 5. https://doi.org/10.24198/farmasetika.v2i5.16780

Tao M, Kruhlak M, Xia S, Androphy E and Zheng Z -M. (2003). Signals that dictate nuclear localization of human papillomavirus type 16 oncoprotein E6 in living cells. *Journal of Virology 77*(24): 13232–13247. https://doi.org/10.1128/JVI.77.24.13232-13247.2003

Trott O and Olson A J. (2009). AutoDock Vina: Improving the speed and accuracy of docking with a new scoring function, efficient optimization, and multithreading. *Journal of Computational Chemistry 31*(2): 455–461. https://doi.org/10.1002/jcc.21334

Tummers B and van der Burg S. (2015). High-risk human papillomavirus targets crossroads in immune signaling. *Viruses 7*(5): 2485–2506. https://doi.org/10.3390/v7052485

Tyring S, Moore A. Y and Lupi O. (2016). *Mucocutaneous manifestations of viral diseases: An illustrated guide to diagnosis and management*. CRC Press.

Umaru I J, Umaru K I and Umaru H A. (2020). Phytochemical screening, isolation, characterization of bioactive and biological activity of bungkang, (*Syzygium polyanthum*) root-bark essential oil. *Korean Journal of Food & Health Convergence 6*(3): 18.

Underbrink M P, Dupuis C, Wang J and Tyring S K. (2016). E6 proteins from low-risk human papillomavirus types 6 and 11 are able to protect keratinocytes from apoptosis via Bak

degradation. *The Journal of General Virology 97*(3): 715–724. https://doi.org/10.1099/jgv.0.000392

Van Doorslaer K and Burk R D. (2010). Evolution of human papillomavirus carcinogenicity. *Advances in Virus Research 77*: 41–62. https://doi.org/10.1016/B978-0-12-385034-8.00002-8

Vande Pol S B and Klingelhutz A J. (2013). Papillomavirus E6 oncoproteins. *Virology 445*(1): 115–137. https://doi.org/10.1016/j.virol.2013.04.026

Wahidin M, Febrianti R and Susanty F. (2020). *Burden of cervical cancer in Indonesia: Findings from the global burden of disease study 1990–2017*, 213–217. https://doi.org/10.2991/ahsr.k.200215.040

Wang X, Huang X and Zhang Y. (2018). Involvement of human papillomaviruses in cervical cancer. *Frontiers in Microbiology 9*: 1–14. https://doi.org/10.3389/fmicb.2018.02896

Wei J -N, Liu Z -H, Zhao Y-P, Zhao L -L, Xue T -K and Lan Q -K. (2019). Phytochemical and bioactive profile of Coriandrum sativum L. *Food Chemistry 286*: 260–267. https://doi.org/10.1016/j.foodchem.2019.01.171

Westrich J A, Warren C J and Pyeon D. (2017). Evasion of host immune defenses by human papillomavirus. *Virus Research 231*: 21–33. https://doi.org/10.1016/j.virusres.2016.11.023

White E A, Walther J, Javanbakht H and Howley P M. (2014). Genus beta human papillomavirus E6 proteins vary in their effects on the transactivation of p53 target genes. *Journal of Virology 88*(15): 8201–8212. https://doi.org/10.1128/JVI.01197-14

Widiastuti D, Warnasih S, Sinaga S E, Pujiyawati E, Supriatno and Putra W E. (2023). Identification of active compounds from *Averrhoa bilimbi* L. (Belimbing Wuluh) flower using LC-MS and antidiabetic activity test using in vitro and in silico approaches. *Trends in Sciences 20*(8): 1-9. https://doi.org/10.48048/tis.2023.6761

Woerdenbag H J and Kayser O. (2014). Jamu: Indonesian traditional herbal medicine towards rational phytopharmacological use. *Journal of Herbal Medicine 4*(2): 51–73.

Yahia Y, Benabderrahim M A, Tlili N, Bagues M and Nagaz K. (2020). Bioactive compounds, antioxidant and antimicrobial activities of extracts from different plant parts of two Ziziphus Mill. Species. *Plos One 15*(5): e0232599. https://doi.org/10.1371/journal.pone.0232599

Zahra S and Iskandar Y. (2017). Review artikel: Kandungan senyawa kimia dan bioaktivitas *Ocimum basilicum* L. *Farmaka 15*(3): 3. https://doi.org/10.24198/jf.v15i3.13770

Zanier K, Stutz C, Kintscher S, Reinz E, Sehr P, Bulkescher J, Hoppe-Seyler K, Travé G and Hoppe-Seyler F. (2014). The E6AP binding pocket of the HPV16 E6 oncoprotein provides a docking site for a small inhibitory peptide unrelated to E6AP, indicating druggability of E6. *PloS One 9*(11): 1–12. https://doi.org/10.1371/journal.pone.0112514

Zhang S, Xu H, Zhang L and Qiao Y. (2020). Cervical cancer: Epidemiology, risk factors and screening. *Chinese Journal of Cancer Research 32*(6): 720–728. https://doi.org/10.21147/j.issn.1000-9604.2020.06.05

Zhao Y, Zeng C and Massiah M A. (2015). Molecular dynamics simulation reveals insights into the mechanism of unfolding by the A130T/V mutations within the MID1 Zinc-binding Bbox1 domain. *PloS One 10*(4): e0124377. https://doi.org/10.1371/journal.pone.0124377